Bulletin of Mathematical Biology (2007) 69: 1691–1708
DOI 10.1007/s11538-006-9186-5

ORIGINAL ARTICLE

A Microenvironment Based Model of Antimitotic Therapy of Gompertzian Tumor Growth

Frank Kozusko[a,*], Michele Bourdeau[b], Zeljko Bajzer[c], David Dingli[d,e,*]

[a] *Department of Mathematics, Hampton University, Hampton, VA 23668, USA*
[b] *Lehman Brothers, New York, NY 10019, USA*
[c] *Biomathematics Resource, Mayo Clinic College of Medicine, Rochester, MN 55905, USA*
[d] *Division of Hematology, Mayo Clinic College of Medicine, Rochester, MN 55905, USA*
[e] *Program for Evolutionary Dynamics, Harvard University, One Brattle Square, Ste 6, Cambridge, MA 02138, USA*

Received: 21 August 2006 / Accepted: 2 November 2006 / Published online: 15 February 2007

Abstract A model of tumor growth, based on two-compartment cell population dynamics, and an overall Gompertzian growth has been previously developed. The main feature of the model is an inter-compartmental transfer function that describes the net exchange between proliferating (P) and quiescent (Q) cells and yields Gompertzian growth for tumor cell population $N = P + Q$. Model parameters provide for cell reproduction and cell death. This model is further developed here and modified to simulate antimitotic therapy. Therapy decreases the reproduction-rate constant and increases the death-rate constant of proliferating cells with no direct effect on quiescent cells. The model results in a system of two ODE equations (in N and P/N) that has an analytical solution. Net tumor growth depends on support from the microenvironment. Indirectly, this is manifested in the transfer function, which depends on the proliferation ratio, P/N. Antimitotic therapy will change P/N, and the tumor responds by slowing the transfer rate from P to Q. While the cellular effects of therapy are modeled as dependent only on antimitotic activity of the drug, the tumor response also depends on the tumor age and any previous therapies—*after therapy, it is not the same tumor*. The strength of therapy is simulated by the parameter λ, which is the ratio of therapy induced net proliferation rate constant versus the original. A pharmacodynamic factor inversely proportional to tumor size is implemented. Various chemotherapy regimens are simulated and the outcomes of therapy administered at different time

*Corresponding author.
E-mail addresses: frank.kozusko@hamptonu.edu (F. Kozusko), dingli.david@mayo.edu (D. Dingli)

points in the life history of the tumor are explored. Our analysis shows: (1) for a constant total dose administered, a decreasing dose schedule is marginally superior to an increasing or constant scheme, with more pronounced benefit for faster growing tumors, (2) the minimum dose to stop tumor growth is age dependent, and (3) a dose-dense schedule is favored. Faster growing tumors respond better to dose density.

Keywords Gompertz · Chemotherapy · Cell kinetics · Proliferation · Tumor

1. Introduction

Cancer therapy has been the target of mathematical modeling for many decades. The models have evolved in complexity as our understanding of cancer biology has expanded. The simplest models were based on Gompertzian growth (Norton and Simon, 1986; Sullivan, 1972; Norton et al., 1976; Wheldon, 1988; de Vladar and Gonzalez, 2004; Norton, 2005) that nonetheless allowed predictions for optimization of therapy. More complex models have taken into consideration some biologically understood principles relating to cell cycle kinetics and cell–cell interactions, age-structured cell populations, vasculature, spatial distribution of cells, pharmacodynamics and pharmacokinetics (Wheldon, 1988; Cojocaru and Agur, 1992; Panetta, 1995, 1996, 1997; Jackson and Byrne, 2000; Kozusko et al., 2001; Dyson et al., 2002; Bertuzzi et al., 2003; Panetta et al., 2003; Sidorov et al., 2003; Ribba et al., 2005; Magni et al., 2006). Such complex models usually involve considerable computational effort, and require many parameters to be estimated or considered for optimization.

In the present paper, we propose a generic model for antimitotic cancer therapy that can be relatively easily used for treatment optimization, and yet this model is more sophisticated than the simple empirical models (Sullivan, 1972; Norton and Simon, 1977, 1986). It includes cell kinetics with two basic cell subpopulations (proliferating and quiescent), sigmoidal (not just exponential) growth of the unperturbed tumor, and one-parameter characterization of the effect of therapy. The model has a relatively simple analytical solution and consequently offers advantages for quick investigation of treatment regimens.

The unperturbed tumor growth is modeled by choosing the net exchange rate between proliferating (P) and quiescent (Q) cells in such a way that it yields empirically established Gompertzian growth for the total cell population (Kozusko and Bajzer, 2003). The net exchange rate between P and Q is assumed to be a characteristic of the tumor and its microenvironment, and thus, represents the cumulative response of the tumor to nutrient and oxygen supply and intercellular communication. Therapy is assumed to change the reproduction and death rate constants of cells in the proliferating compartment. The net exchange rate is influenced by therapy through its dependence on the proliferation ratio, which is altered by therapy. Two important implications of the model are that the tumor response to antimitotic therapy depends on the age of the tumor and on previous therapy. This means that after each treatment cycle, the tumor changes its growth kinetics.

Table 1 Gompertz parameters for a selected group of tumors

	k_+ (per year)	k_- (per year)	k_+ / k_-	t_i (y)
Parathyroid (a)	2.76	0.134	20.6	22.6
Parathyroid (b)	6.47	0.314	20.6	9.6
Myeloma	126	4.41	28.6	0.8
Testicular	112	4.52	24.8	0.7

Note. Data taken from Parfitt and Fyhrie (1997).

In order to illustrate the potential of this model, we have simulated a number of antimitotic therapy regimens and analyzed their outcomes for a general spectrum of Gompertzian tumors. Specific examples are provided for Gompertzian tumors identified in the literature (Table 1). There are a few, somewhat surprising results, but for the most part the outcomes are in agreement with clinical findings (Bonadonna et al., 1995, 2004; Citron et al., 2003; Pfreundschuh et al., 2004a,b). In particular, dose-dense therapy is shown to give higher tumor reductions compared to a fixed-dose regimen and faster growing tumors are more sensitive to antimitotic therapy. Moreover, the results clearly show that it is not possible to cure a tumor with cell cycle specific therapy alone.

2. The Gompertz growth model

The cell population dynamics model that produces Gompertz growth was presented in Kozusko and Bajzer (2003). It is briefly reviewed and reformulated here (a summary of parameter definitions is provided in Table 2). The normalized Gompertz function is

$$N(t) = \exp\left\{\frac{k_+}{k_-}\left(1 - e^{-k_- t}\right)\right\}, \quad N(0) = 1, \tag{1}$$

and satisfies the equation

$$\dot{N} = k_+ N - k_- N \ln(N), \quad N(0) = 1 \Rightarrow \frac{\dot{N}}{N} = k_+ - k_- \ln(N). \tag{2}$$

The model presented in Fig. 1 produces the following cell population dynamics equations:

$$\dot{P} = (\beta - \mu_P) P - \Phi(N). \tag{3}$$

$$\dot{Q} = \Phi(N) - \mu_Q Q \tag{4}$$

$$N = P + Q, \quad P(0) + Q(0) = P_0 + Q_0 = 1$$

where P and Q are the proliferating and quiescent (non-proliferating) cells, respectively. $\Phi(N)$ is the net inter-compartmental transfer function and is positive if the net transition is from the proliferating to the quiescent compartment. In Kozusko

Table 2 Definition of Parameters

D	Modeling parameter ($D^2 \equiv [(1+\gamma)/2]^2 - \gamma(P/N)_\infty$)
k_+	Growth rate constant in Gompertz model of tumor growth
k_-	Retardation of growth constant in Gompertz model of tumor growth
m	Parameter for Gompertz tumor growth ($m \equiv \beta - \mu_P + \mu_Q$)
$\bar{m}$	Parameter for antimitotic therapy ($\bar{m} \equiv \bar{\beta} - \bar{\mu}_P + \mu_Q$)
N	Total number of cells ($N = P + Q$)
N_{C0}	Value of total number of cells at start of each chemotherapy cycle
N_{G0}	Value of N at start of each subsequent rest period after cessation of chemotherapy
N_{t_I}	Undisturbed tumor size at the inflection point (maximum growth rate) of Gompertz tumor growth
N_∞	Size of undisturbed Gompertz tumor growth at $t \to \infty$ ($N_\infty = \exp(k_+/k_-)$)
P	Number of proliferating cells
P/N	Proliferation ratio
$(P/N)_{C0}$	Value of proliferation ratio at start of each chemotherapy cycle
$(P/N)_{G0}$	Value of proliferation ratio, P/N, at start of each subsequent rest period following the cessation of chemotherapy
$(P/N)_G$	Value of proliferation ratio, P/N, for undisturbed Gompertzian tumor growth
$(P/N)_\infty$	Limiting value for proliferating ratio for undisturbed tumor as $t \to \infty$ ($(P/N)_\infty \equiv \mu_Q/m$)
Q	Number of quiescent cells
t_I	Tumor age at inflection point for undisturbed Gompertz tumor growth
t_G	Age of tumor when therapy is commenced
β	Proliferation rate parameter
γ	Modeling parameter ($\gamma \equiv k_-/m(1-\lambda)$)
$\lambda \equiv \bar{m}/m$	Modeling parameter related to "relative" strength of antimitotic therapy ($\lambda \equiv \bar{m}/m < 1$)
μ_P	Death rate parameter for proliferating cells P
μ_Q	Death rate parameter for quiescent cells Q
$\Phi(N)$	Net inter-compartmental transfer function
$\Psi(P/N)$	$\Phi(N) = N\Psi(P/N)$

and Bajzer (2003), it was shown that $\Phi(N)$ is always positive during Gompertz growth. $\mu_P > 0$ and $\mu_Q > 0$ represent the death rate parameters for the proliferating and quiescent compartments, respectively. $\beta > 0$ is the proliferation or reproduction rate parameter. Growth requires that $\beta - \mu_P > 0$. Adding Eqs. (3) and (4) and defining $m \equiv \beta - \mu_P + \mu_Q$ yields

$$\dot{P} = (m - \mu_Q)P - \Phi(N) \tag{5}$$

$$\dot{N} = mP - \mu_Q N. \tag{6}$$

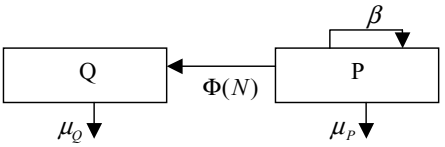

Fig. 1 The tumor population has both proliferating (P) and quiescent (Q) cells conceptually in separate compartments. During Gompertzian growth, net transfer of cells is always from P to Q and $\Phi(N)$ is positive.

As $t \to \infty$, $\dot{N}, \dot{P} \to 0 \Rightarrow (P/N)_\infty \equiv \mu_Q/m$. Anticipating the form of $\Phi(N)$ as $\Phi(N) = N\,\Psi(P/N)$, Eqs. (5) and (6) can be written as

$$\frac{\dot{P}}{N} = m\left\{1 - \left(\frac{P}{N}\right)_\infty\right\}\left(\frac{P}{N}\right) - \Psi\left(\frac{P}{N}\right) \tag{7}$$

$$\frac{\dot{N}}{N} = m\left\{\left(\frac{P}{N}\right) - \left(\frac{P}{N}\right)_\infty\right\}. \tag{8}$$

Here we make the fundamental assumption that the tumor growth is Gompertzian and described by Eq. (2). Equating Eqs. (8) and (2) one gets

$$k_+ - k_- \ln(N) = m\left\{\left(\frac{P}{N}\right) - \left(\frac{P}{N}\right)_\infty\right\}. \tag{9}$$

Differentiating Eq. (9), and using the substitutions provided by Eqs. (7) and (8) provides

$$\Psi\left(\frac{P}{N}\right) = -m\left(\frac{P}{N}\right)^2 + \{m + k_-\}\left(\frac{P}{N}\right) - k_-\left(\frac{P}{N}\right)_\infty. \tag{10}$$

Assuming as in Kozusko and Bajzer (2003) that the initial cell population is entirely proliferating, we equate Eqs. (2) and (6) at $t = 0$ and $N(0) = P(0) = 1$, $Q(0) = 0$, then $\beta - \mu_P = k_+$ and Eq. (10) can be represented as

$$\Psi\left(\frac{P}{N}\right) = -(k_+ + \mu_Q)\left(\frac{P}{N}\right)^2 + \{k_+ + \mu_Q + k_-\}\left(\frac{P}{N}\right) - k_-\left(\frac{P}{N}\right)_\infty. \tag{11}$$

While k_+ and μ_Q relate to the individual cell kinetics (which in themselves may relate to the tumor as a whole), k_- is strictly a whole tumor, microenvironment-based parameter arising from $\Psi(P/N)$.

3. Model for antimitotic therapy

We now make adjustments to the system of cell population dynamics Eqs. (7) and (8) to simulate antimitotic therapy. From here onwards, we will assume chemotherapy, noting that the model applies to any therapy directed against actively replicating cells. Our first modeling assumption is that $\Psi(P/N)$ represents the cumulative response of the tumor to nutrient and oxygen supply and intercellular communication. $\Psi(P/N)$ is assumed to be fundamental to the given tumor behavior in its microenvironment as represented by the values of k_+, k_- and μ_Q. We expect $\Psi(P/N)$ will remain the same function Eq. (11) with changes resulting from chemotherapy reflected in (P/N).

We assume that an antimitotic drug will reduce the reproduction factor β and increase the death rate μ_P of proliferating cells, but will have no effect on

μ_Q:$(\beta - \mu_P) \rightarrow (\bar{\beta} - \bar{\mu}_P)$ and $m \rightarrow \overline{m}$. We define $\lambda \equiv (\bar{m}/m) < 1$ as a modeling parameter. If the antimitotic effect is significant enough to greatly reduce the reproduction factor β and increase the proliferating cell death rate μ_P then, $\lambda < 0$. Although λ cannot be related directly to the strength of the drug, it can be used in a relative evaluation. If the drug effect is assumed to be linear with the drug concentration (e.g., doubling the concentration doubles $\overline{m} < 0$) then, doubling $\lambda < 0$ is equivalent to doubling the drug concentration modeled. The system of equations for chemotherapy is

$$\dot{P} = (m\lambda - \mu_Q)P - N\Psi(N) = m\left(\lambda - \left(\frac{P}{N}\right)_\infty\right)P - N\Psi\left(\frac{P}{N}\right) \tag{12}$$

$$\dot{N} = m\lambda P - \mu_Q N = m\left(\lambda P - \left(\frac{P}{N}\right)_\infty N\right) \tag{13}$$

or

$$\frac{\dot{P}}{N} = m\left\{\lambda - \left(\frac{P}{N}\right)_\infty\right\}\left(\frac{P}{N}\right) - \Psi\left(\frac{P}{N}\right) \tag{14}$$

$$\frac{\dot{N}}{N} = m\left\{\lambda\left(\frac{P}{N}\right) - \left(\frac{P}{N}\right)_\infty\right\}. \tag{15}$$

Using

$$\frac{d\,(P/N)}{dt} = \frac{\dot{P}}{N} - \left(\frac{P}{N}\right)\left(\frac{\dot{N}}{N}\right)$$

and Eqs. (10), (13) and (14) produces

$$\frac{d\,(P/N)}{dt} = m(1-\lambda)\left\{\left(\frac{P}{N}\right)^2 - [1+\gamma]\left(\frac{P}{N}\right) + \gamma\left(\frac{P}{N}\right)_\infty\right\}$$

$$\gamma \equiv \frac{k_-}{m(1-\lambda)}. \tag{16}$$

The integration of this equation has three possible solutions but parameter analysis eliminates two of the possibilities (see Appendix). The remaining solution is:

$$\left(\frac{P}{N}\right) = \frac{1+\gamma}{2} - D \cdot \tanh\left[Dm(1-\lambda)\,(t + C_I)\right], \tag{17}$$

$$C_I = \left(\frac{-1}{2Dm(1-\lambda)}\right)\ln\left\{\frac{D + [(P/N)_{C0} - (1+\gamma)/2]}{D - [(P/N)_{C0} - (1+\gamma)/2]}\right\};$$

$$D^2 \equiv \left(\frac{1+\gamma}{2}\right)^2 - \gamma\left(\frac{P}{N}\right)_\infty. \tag{18}$$

Here, $(P/N)_{C0}$ is the value of (P/N) at the start of each chemotherapy cycle.

Substituting Eq. (17) into Eq. (15) and integrating yields

$$N = N_{C0} \exp\left\{m\left[\frac{\lambda(1+\gamma)}{2} - \left(\frac{P}{N}\right)_\infty\right]t\right\} \cdot \left\{\frac{\cosh[Dm(1-\lambda)C_I]}{\cosh[Dm(1-\lambda)(t+C_I)]}\right\}^{\frac{\lambda}{1-\lambda}}. \tag{19}$$

Here, N_{C0} is the value of N at the start of each chemotherapy cycle.

To determine the tumor behavior between chemotherapy cycles, we evaluate Eqs. (15) and (16) at $\lambda = 1$, which corresponds to the drug-free interval

$$\frac{d(P/N)}{dt} = -k_-\left\{\left(\frac{P}{N}\right) - \left(\frac{P}{N}\right)_\infty\right\} \Rightarrow$$

$$\left(\frac{P}{N}\right) = \left[\left(\frac{P}{N}\right)_{G0} - \left(\frac{P}{N}\right)_\infty\right]e^{-k_- t} + \left(\frac{P}{N}\right)_\infty \tag{20}$$

$$\frac{\dot{N}}{N} = m\left\{\left(\frac{P}{N}\right) - \left(\frac{P}{N}\right)_\infty\right\} \tag{21}$$

$$N(t) = N_{G0} \exp\left\{\frac{\hat{k}_+}{k_-}(1 - e^{-k_- t})\right\}, \quad \hat{k}_+ \equiv m\left\{\left(\frac{P}{N}\right)_{G0} - \left(\frac{P}{N}\right)_\infty\right\}, \tag{22}$$

where N_{G0} and $(P/N)_{G0}$ are the values at the start of each subsequent rest period after cessation of chemotherapy. Here, we see that the tumor resumes Gompertzian growth after each chemotherapy cycle, but with a new $\hat{k}_+$ determined by the reset (P/N) ratio. (For the analysis that follows, we define the chemotherapy as successful if the tumor has a zero or negative growth rate at the end of the last cycle.) If the final $(P/N)_{G0} > (P/N)_\infty$, the chemotherapy is not successful, and the tumor will resume growth to a new but lower N_∞ than would have existed without the chemotherapy. If the regime is successful (the final $(P/N)_{G0} < (P/N)_\infty$), the tumor will continue to decrease in size to a new lower equilibrium.

4. Discussion

4.1. The reduced Growth and chemotherapy systems

It is interesting to compare this model to those that are frequently used to simulate chemotherapy events (Norton and Simon, 1986; Wheldon, 1988; Byrne, 2003). The usual ODE representations of tumor growth and chemotherapy are given respectively by

$$\dot{N} = [k_+ - k_- \ln(N)]\,N \quad \text{and} \quad \dot{N} = [k_+ - k_- \ln(N)]\,N - C(\mu, t, N)N, \tag{23}$$

where $C(\mu, t, N)N$ is a cell-kill term representing a change to the rate equation as a result of antimitotic therapy and μ is the killing-rate constant. Functional

dependence on t arises from the drug concentration profile in time. To conform with the standard treatment practices we have introduced the time dependence in our model by assuming a piecewise constant drug concentration. Our model emphasizes the ratio (P/N) as an important component of both growth and chemotherapy. Our system of equations can be shown to take the following forms:

Growth:

$$\frac{dN}{dt} = m\left\{\left(\frac{P}{N}\right) - \left(\frac{P}{N}\right)_{\infty}\right\} N; \quad \frac{d(P/N)}{dt} = -k_{-}\left\{\left(\frac{P}{N}\right) - \left(\frac{P}{N}\right)_{\infty}\right\}. \quad (24)$$

Antimitotic therapy:

$$\frac{dN}{dt} = m\left\{\left(\frac{P}{N}\right) - \left(\frac{P}{N}\right)_{\infty}\right\} N - m(1-\lambda)\left(\frac{P}{N}\right) N$$

$$\frac{d(P/N)}{dt} = -k_{-}\left\{\left(\frac{P}{N}\right) - \left(\frac{P}{N}\right)_{\infty}\right\} - m(1-\lambda)\left\{1 - \left(\frac{P}{N}\right)\right\}\left(\frac{P}{N}\right). \quad (25)$$

Our reduced form (similar to Eq. (23)) is:

Growth:

$$\frac{dN}{dt} = G_1\left(\frac{P}{N}\right) N; \quad \frac{d(P/N)}{dt} = -G_2\left(\frac{P}{N}\right). \quad (26)$$

Antimitotic therapy:

$$\frac{dN}{dt} = G_1\left(\frac{P}{N}\right) N - C_1\left(\lambda, \left(\frac{P}{N}\right)\right) N$$

$$\frac{d(P/N)}{dt} = -G_2\left(\frac{P}{N}\right) - C_2\left[\lambda, \left(\frac{P}{N}\right)\right]\left(\frac{P}{N}\right), \quad (27)$$

where $C_1(\lambda, (P/N))$ and $C_2(\lambda, (P/N))$ represent therapy induced changes to the rate equations. They are dependent on the applied dose λ and the sensitivity of the tumor to chemotherapy (a function of P/N) resulting partly from the microenvironment. We note that

$$C_1\left(\lambda, \frac{P}{N}\right) = m(1-\lambda)\left(\frac{P}{N}\right) = (m - \bar{m})\left(\frac{P}{N}\right) = \Delta m\left(\frac{P}{N}\right)$$

and

$$C_2\left(\lambda, \frac{P}{N}\right) = m(1-\lambda)\left\{1 - \left(\frac{P}{N}\right)\right\} = \Delta m\left(\frac{Q}{N}\right).$$

Then, the growth rate of N is altered by the change in P/N as might be expected and the growth rate of (P/N) by changes in Q/N.

4.2. Comparison of systems

Equation (23) assumes that all Gompertzian growth tumors with the same k_+ and k_- are the same. There is no accounting for the size of the proliferating cell compartment, ultimately represented by the (P/N) ratio. It has been shown (Kozusko and Bajzer, 2003) that this ratio depends on μ_Q as

$$\left(\frac{P}{N}\right) = \frac{\mu_Q + k_+ e^{-k_- t}}{\mu_Q + k_+} = \left(\frac{P}{N}\right)_\infty + \frac{k_+ e^{-k_- t}}{\mu_Q + k_+}. \tag{28}$$

Additionally, after any antimitotic chemotherapy, (P/N) has been reduced such that it is no longer consistent with that expected for an untreated tumor of the same size. Therefore, the tumor growth rate is slower. Clearly, after the tumor receives therapy, it is *not the same tumor* and Eq. (23) cannot be reapplied. Equations (24) through (27) show the importance of the (P/N) ratio to the growth and chemotherapy-effected systems. Equation (18) shows that each subsequent chemotherapy response is dependent on the previous history of growth and decay as represented in the term $(P/N)_{C0}$, as well as the resulting tumor size, N_{C0}.

4.3. Effective versus ineffective chemotherapy

Equation (22) predicts the tumor growth behavior at the end of any antimitotic therapy. If chemotherapy is effective, the (P/N) ratio will have been reduced to less than $(P/N)_\infty$, then, $\hat{k}_+ = m\{(P/N)_{G0} - (P/N)_\infty\}$ is negative and the tumor will decay. If the chemotherapy is ineffective the tumor will resume growth.

After the last cycle of antimitotic therapy, the tumor will grow or decay to a new equilibrium level, which is smaller than that of the unaffected tumor, $N_\infty(C) < N_\infty(G)$

$$N_\infty(C) < N_\infty(G) \exp\left\{\frac{m\{(P/N)_{G0} - (P/N)_G\}}{k_-}\right\}, \tag{29}$$

where $(P/N)_{G0}$ is the proliferation ratio at the completion of the last antimitotic therapy, which will be less than that of the unaffected tumor of $(P/N)_G$ of the same size. Depending on the value of $(P/N)_{G0}$, $N_\infty(C)$ may be larger than N_{G0} and the tumor will continue to grow, however, if $N_\infty(C)$ is smaller than N_{G0} the tumor will decay after cessation of therapy. For ineffective therapy, (P/N) will decay to $(P/N)_\infty$ while N increases; for effective therapy (P/N) will grow to $(P/N)_\infty$ while N decreases.

4.4. The significance of the transfer function and $(P/N)_\infty$

The tumor responds to therapy by reducing the $P \to Q$ transfer. During the therapy interval, (P/N) is reduced. Simple analysis of the parabolic transfer function shows (see Eq. (10)) that $\Psi(P/N)$ decreases with decreasing (P/N) and is still positive when $(P/N) = (P/N)_\infty$. For therapy to be effective, the (P/N) ratio must fall

below $(P/N)_\infty$ by the end of the last therapy cycle (see Eq. (22)). While $\Psi(P/N)$ may still be positive, the $P \rightarrow Q$ transfer is decreased and the Q compartment continues to lose cells by factor μ_Q. The Q compartment will decrease allowing a fractional decrease of N greater than the (P/N) ratio at the start of chemotherapy: i.e. $\Delta N/N > (P/N_{C0})$. If therapy is strong enough, (P/N) may decrease enough to cause $\Psi(P/N)$ to become negative and a $Q \rightarrow P$ transfer will take place. This increases the target cell population while simultaneously decreasing the Q compartment with further reduction in the size of the tumor.

5. Simulations

We will use Eqs. (17)–(22) to model the changes in N and (P/N) during the modeled chemotherapy regime, which is (unless otherwise stated) 8 hours of chemotherapy every 3 weeks for six cycles. We use $\mu_Q = 1$ and indicated values of k_+ and k_-. λ, which is modeled as constant during each 8-hours cycle, will be the parameter that represents the strength or concentration of the antimitotic drug, t_G is the age of the tumor at the commencement of chemotherapy, $t_I = \ln(k_+/k_-)/k_-$ (see Kozusko and Bajzer, 2003) is the age of the tumor at the inflection point (maximum growth rate). Table 1 provides rate parameters and is taken from Table 4 in Parfitt and Fyhrie (1997).

In order to model the efficacy of the drug versus the size of the tumor, we apply a pharmacodynamic factor to λ. At the beginning of each chemotherapy cycle, λ is multiplied by the ratio N_{t_I}/N, where N_{t_I} is the undisturbed tumor size at the inflection point and N is the current tumor size. This produces an effective λ: $\lambda_{\text{eff}} = \lambda(N_{t_I}/N)$, which is inversely proportional to N and normalized to the inflection point.

As a preliminary to therapy simulations, we briefly recall the system trends of the unperturbed-Gompertz growth tumor (Kozusko and Bajzer, 2003): N and Q increase to N_∞ and Q_∞; $\Phi = N\Psi(P/N)$ goes through a maximum after $t_G = t_I$ and then decreases to Φ_∞; P may peak before approaching P_∞ and (P/N) continually decays to $(P/N)_\infty$.

Figure 2 is presented as an example to show the overall system response when the modeled therapy regimen is effective. The example is for a parathyroid tumor (a), $\lambda = -8$. Time zero corresponds to the start of the first cycle of therapy. Figure 2c and d show the expected decreases in P and (P/N) during therapy. This leads to a reduction in the $P \rightarrow Q$ transfer observed in Fig. 2b. The Q compartment continues to grow but at a slower rate because of the decreased cell transfer with continued μ_Q losses (Fig. 2a). The size of N decreases during therapy but increases again during the rest periods (Fig. 2a). Finally we note that (P/N) decreases below $(P/N)_\infty$ during the last therapy cycle. This produces the continual decay of N, Q and P, while (P/N) restores to $(P/N)_\infty$.

In contrast, an ineffective chemotherapy regimen is presented in Fig. 3 to be compared with Fig. 2. The example is for parathyroid carcinoma (a), $\lambda = -5$. In Figs. 3c and d, we see that P/N and P do not decrease as much during therapy and P recovers more during the rest periods. This leads to faster tumor (N) recovery during the rest periods seen in Fig. 3a. The smaller decreases in P/N lead to smaller

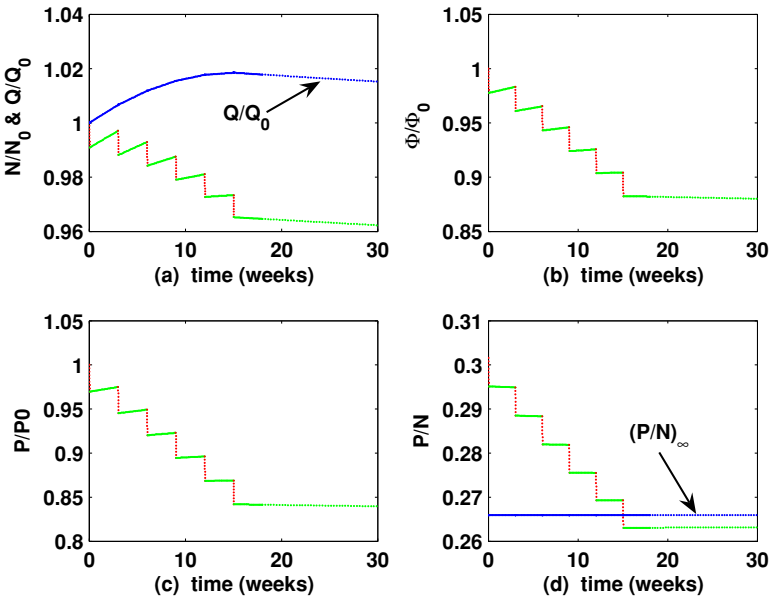

Fig. 2 Effective antimitotic chemotherapy for a parathyroid tumor. Model parameters are $k_+ = 2.76\ \text{year}^{-1}$, $k_- = 0.134\ \text{year}^{-1}$, and $\lambda = -8$. Therapy is simulated at the inflection point.

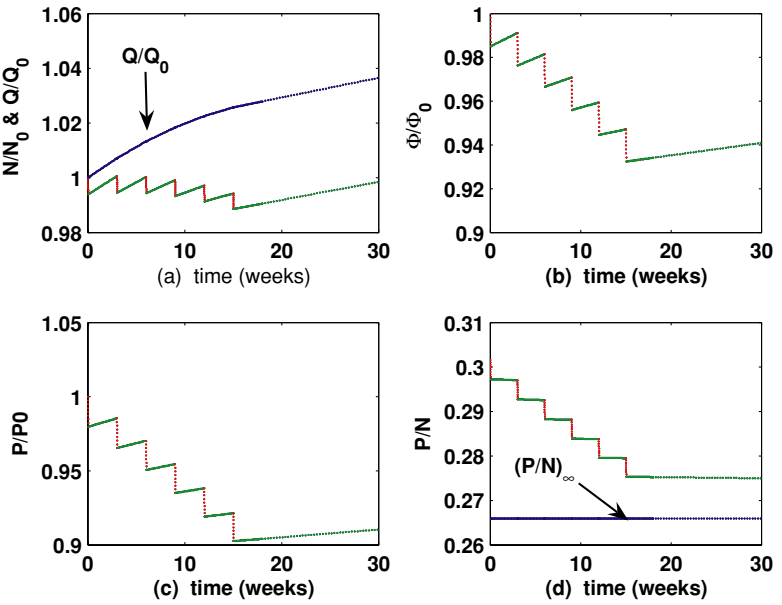

Fig. 3 Ineffective antimitotic chemotherapy on a parathyroid tumor. Model parameters are $k_+ = 2.76\ \text{year}^{-1}$, $k_- = 0.134\ \text{year}^{-1}$ and $\lambda = -5$. Therapy is simulated at the inflection point.

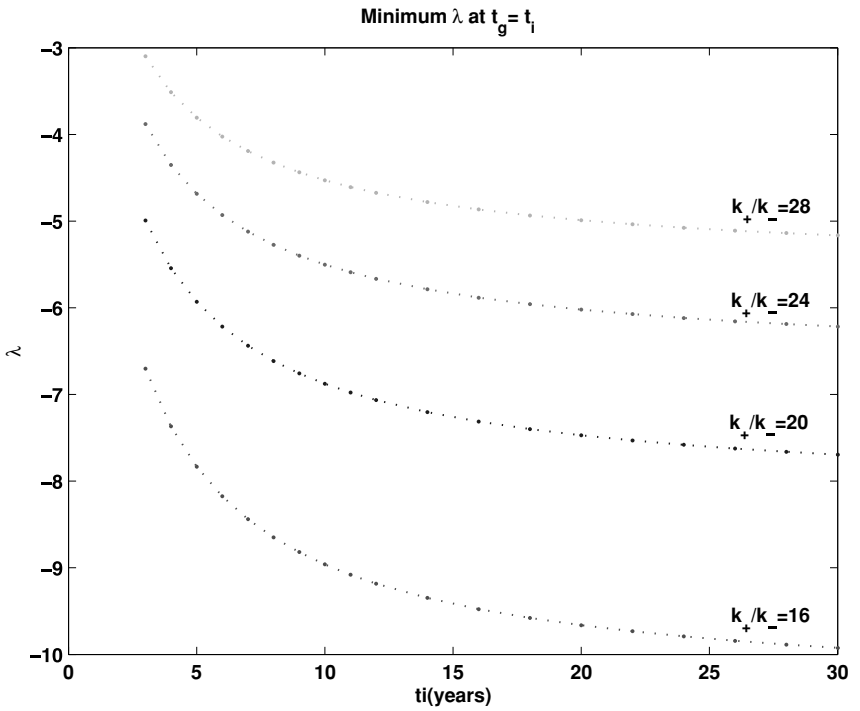

Fig. 4 Minimum λ to stop growth with the model therapy for $t_G = t_I$.

reductions in Φ displayed in Fig. 3b, and therefore, compartment Q continues to grow (Fig 3a). Of course the increase in Q is responsible for the continued expansion of N. Finally, we note (Fig. 3d) that P/N never decreases below $(P/N)_\infty$ which is the ultimate reason why chemotherapy is ineffective.

5.1. Efficacy depends on tumor age

Figures 4 and 5 provide a general overview of the impact of tumor age on the efficacy of antimitotic therapy. The family of curves k_+/k_- relate to the size of the tumor at the inflection point (maximum growth rate) or at $t \to \infty$, since $N_{t_I} = \exp(k_+/k_-)/e = N_\infty/e$ (Kozusko and Bajzer, 2003). The horizontal axis, $t_I = \ln(k_+/k_-)/k_-$, is the tumor age at the inflection point and indirectly indicates k_- and the growth rate of the tumor. In Fig. 4, the vertical axis indicates the minimum value of λ required to stop tumor growth at the completion of the modeled chemotherapy regimen when therapy is commenced at $t_G = t_I$. This graph shows that slower growing tumors require more effective therapy or are less sensitive to antimitotic chemotherapy. As an example: parathyroid (a) and (b) both have $k_+/k_- = 20.6$. The faster growing (b) with $t_I = 9.6$ years requires $\lambda = -6.6$, while (a) with $t_I = 22.6$ years needs $\lambda = -7.3$.

Figure 5 assumes that therapy is commenced one year prior to the age at the inflection point of the tumor and indicates the λ relative to that from Fig. 4, again

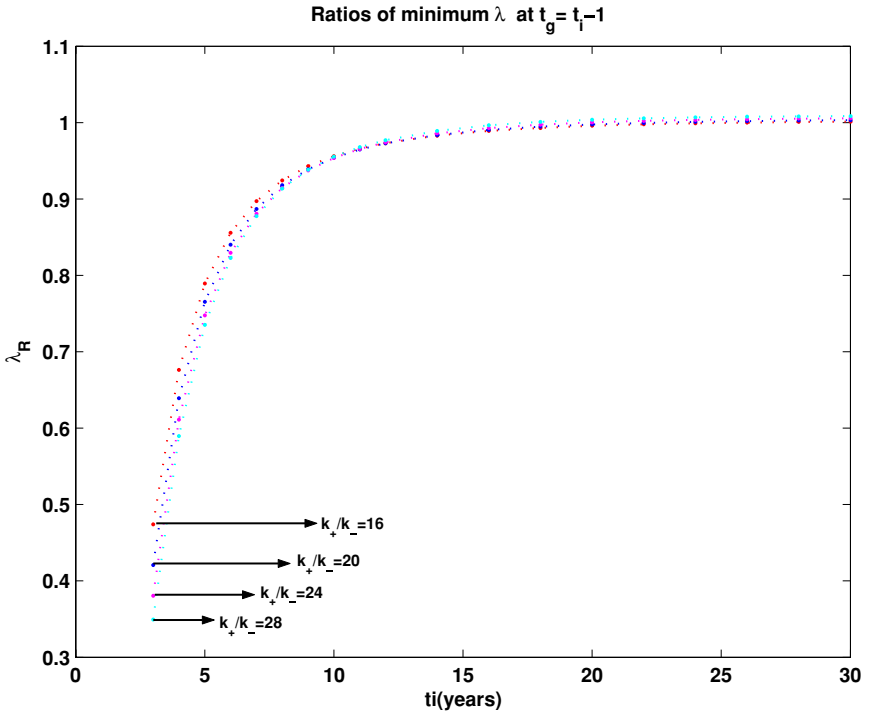

Fig. 5 Fast growing tumors reach the inflection point at a young age. In this figure, therapy is started 1 year before the tumor reaches its maximum growth rate. Rapidly growing tumors are more sensitive to therapy and require a lower λ to stop growth independent of the final carrying capacity.

to stop the growth at completion of the therapy regimen. We can interpret these graphs to mean that faster growing tumors (smallest t_I) are more sensitive to the age of the tumor at commencement of chemotherapy than are slower growing tumors. As an example: parathyroid (a) requires virtually no change in $\lambda(\lambda_R \cong 1.00)$ while the faster growing parathyroid (b) ($\lambda_R = 0.95$ allows a 5% decrease if therapy is commenced one year earlier than the inflection point age. We can also see that the required change in λ is much more sensitive to t_I than it is to the size of the tumor at t_I, that is $\exp(k_+/k_- - 1)$ as represented by the k_+/k_- ratio curves. Figure 6 displays the relative λ for stopping growth in the period $t_G = t_I \pm 3$ years for parathyroid (a) and (b).

5.2. Efficacy depends on therapy distribution

We consider dosing schemes where the total amount of drug delivered for the regimen is constant, but the concentration may vary from one cycle to the next. We compared three different schemes:

(1) *Constant dose scheme*: Each dose is the same (λ_C);

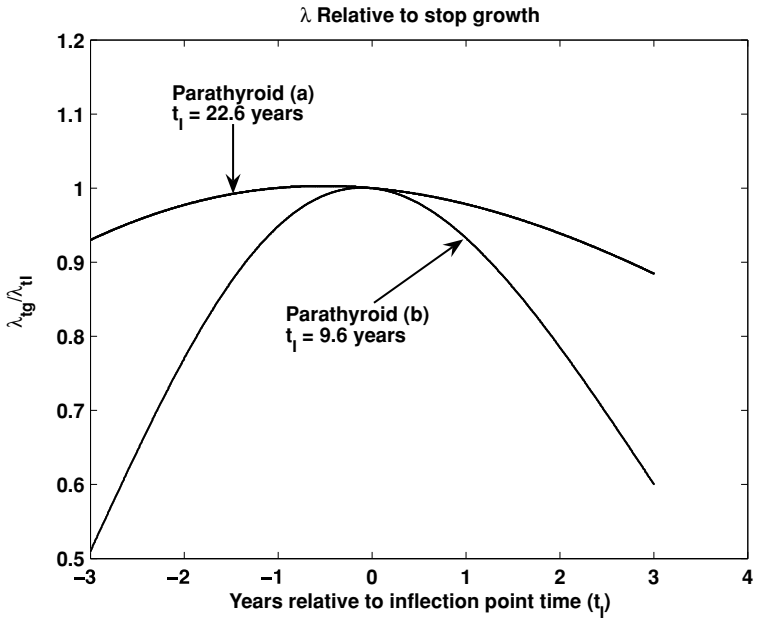

Fig. 6 In this figure, the minimum λ required to stop tumor growth relative to that at the inflection point is studied as a function of time when therapy is started relative to the inflection point.

(2) *Increasing dose scheme*: First dose $0.5\lambda_C$ followed by even steps to $1.5\lambda_C$;
(3) *Decreasing dose scheme*: First dose $1.5\lambda_C$ with even steps to $0.5\lambda_C$.

Our results show that an increasing dose scheme is the least favorable, followed next by the constant dose scheme, with the decreasing dose scheme giving the best results. However, the differences between constant and decreasing dose regimens are small in most cases. The differences are greatest for fast growing tumors when there is a long rest period between therapy cycles. Figure 7 shows the comparison for myeloma ($\lambda_C = -2.5$). In the short term all three schemes allow the tumor to grow past its initial value before decreasing tumor growth. As a general observation, we look at how the efficacy of treatment of the tumor in Fig. 6 might be evaluated. If we look at the constant dose curve and just judge by the size of the tumor, the treatment looks ineffective after three cycles since the tumor has grown. If therapy was terminated, the graph shows that the tumor would continue to grow. Yet just one more cycle would prove to be effective (since the tumor growth shows a negative growth rate after the fourth cycle).

5.3. Efficacy depends on cycle spacing (dose density)

We investigated the outcomes of therapy relative to the time interval between treatment cycles: therapy once per week, once every 2 weeks and once every 3 weeks for the same values of λ, all for six cycles. In general, increasing the dose density (shorter dosing interval) was beneficial but more so for the faster (small t_I)

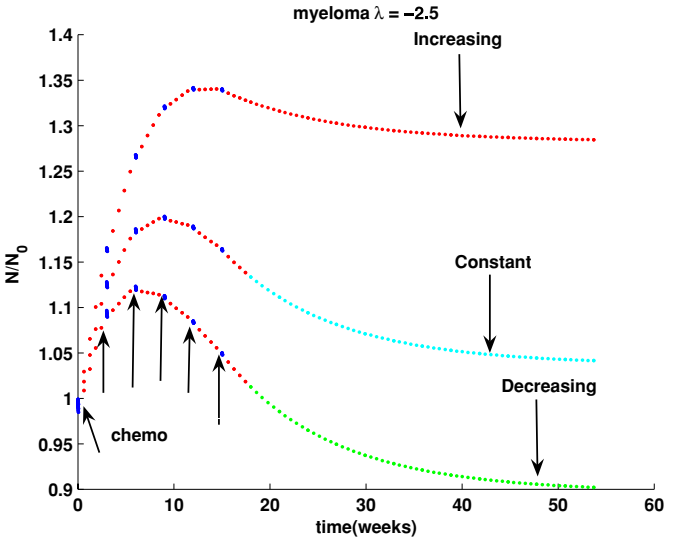

Fig. 7 The rate of tumor growth slowing with therapy depends on how the chemotherapy is dosed. In these simulations, the total dose given over the course of six cycles of therapy is the same. The best response is achieved when the first dose is the highest followed by sequentially decreasing doses. A regimen that starts with a low dose that gradually increases is inferior and the tumor continues to grow despite therapy. The vertical arrows coincide with the timing of therapy.

than for slower growing tumors. Figure 8 displays the expected results for testicular cancer treated at the inflection point (maximum growth rate) for $\lambda = -2.5$. The shorter time intervals between therapy cycles limit the regrowth of the tumor during the rest periods.

6. Conclusion

We have presented a model of Gompertzian tumor growth based on both cell population dynamics parameters (β, μ_P and μ_Q) and the microenvironmental response which is determined by $\Psi(P/N)$ and manifested in the Gompertz parameters k_+ and k_-. We simulated antimitotic chemotherapy by adjusting the cell kinetics parameters that would be affected by this type of therapy. The uniqueness of our system is that tumor growth and therapy response depend on both N and (P/N), not just on the size of the tumor. In fact, we have shown that therapy is only effective if the (P/N) ratio is reduced below $(P/N)_\infty$, otherwise the tumor will regrow between therapy cycles or at the conclusion of therapy. The consideration of both N and (P/N) is most relevant when considering multiple dose therapies. After therapy, it is not the same tumor, since we expect that therapy will have disturbed the Gompertzian growth. Modeling of subsequent therapies must recognize this difference. We propose a system of equations that models the response to cell-cycle-specific therapy of *any* Gompertzian growth tumor. Although we are not able to translate our modeling parameter λ to drug concentration, we have

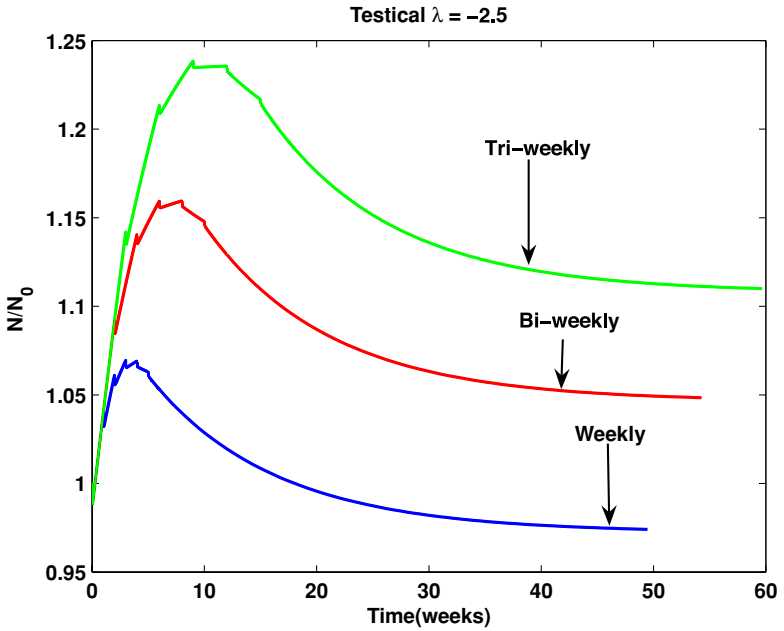

Fig. 8 The frequency of the administration of antimitotic therapy also has an impact on the final tumor volume. Therapy that is given weekly is superior to less time intensive therapy since the tumor can regrow in between cycles of treatment. As in Fig. 7, there is no cure with antimitotic therapy alone.

provided relative comparisons as a function of tumor age, therapy distribution and dosing intervals. We conclude that: (1) the efficacy of antimitotic therapy depends on tumor age but more so for fast growing tumors; (2) for rapidly growing tumors, a therapeutic regimen that starts with a high-dose then decreases with each subsequent cycle is superior to a constant dose regimen which is in turn better than a dose escalation regimen; and (3) dose-dense regimes are beneficial, especially for fast growing tumors.

Appendix: Solution to Equation (16)

Equation (16)

$$\frac{d(P/N)}{dt} = m(1-\lambda)\left\{\left(\frac{P}{N}\right)^2 - [1+\gamma]\left(\frac{P}{N}\right) + \gamma\left(\frac{P}{N}\right)_\infty\right\},$$

$$\gamma \equiv \frac{k_-}{m(1-\lambda)} > 0$$

is of the form

$$\frac{dx}{dt} = cx^2 + bx + a.$$

This equation admits three solutions, depending on the sign of $\Delta = 4ac - b^2$. Solutions are in "tanh()" ($\Delta < 0$), "tan()" ($\Delta > 0$), and "exp()" ($\Delta = 0$). We show below that for our equation

$$\Delta = [m(1-\lambda)]^2 \left\{ 4\gamma \left(\frac{P}{N} \right)_\infty - [1+\gamma]^2 \right\}$$

is always less than zero. Using $m = \beta - \mu_P + \mu_Q = k_+ + \mu_Q$ (see Eq. (11)) and $(P/N)_\infty = \mu_Q/m$, we can expand the above expression and write

$$\begin{aligned} \Delta &= [m(1-\lambda)]^2 \left\{ 4\gamma \left(\frac{m-k_+}{m} \right) - [1+\gamma]^2 \right\} \\ &= [m(1-\lambda)]^2 \left\{ -\frac{4\gamma k_+}{m} - [1-\gamma]^2 \right\} < 0, \end{aligned}$$

and the tanh() is assured.

Acknowledgement

This work was in part supported by grant CA15083 from the NCI (ZB).

References

Bertuzzi, A., D'Onofrio, A., Fasano, A., Gandolfi, A., 2003. Regression and regrowth of tumour cords following single-dose anticancer treatment. Bull. Math. Biol. 65, 903–931.

Bonadonna, G., Zambetti, M., Moliterni, A., Gianni, L., Valagussa, P., 2004. Clinical relevance of different sequencing of doxorubicin and cyclophosphamide, methotrexate, and Fluorouracil in operable breast cancer. J. Clin. Oncol. 22, 1614–1620.

Bonadonna, G., Zambetti, M., Valagussa, P., 1995. Sequential or alternating doxorubicin and CMF regimens in breast cancer with more than three positive nodes. Ten-year results. JAMA 273, 542–547.

Byrne, H.T., 2003. Modeling avascular tumor growth. Cancer modeling and simulation. In: L. Preziosi (Ed.), Chapman & Hall/CRC, New York, pp. 80–86.

Citron, M.L., Berry, D.A., Cirrincione, C., Hudis, C., Winer, E.P., Gradishar, W.J., Davidson, N.E., Martino, S., Livingston, R., Ingle, J.N. et al., 2003. Randomized trial of dose-dense versus conventionally scheduled and sequential versus concurrent combination chemotherapy as postoperative adjuvant treatment of node-positive primary breast cancer: first report of Intergroup Trial C9741/Cancer and Leukemia Group B Trial 9741. J. Clin. Oncol. 21, 1431–1439.

Cojocaru, L., Agur, Z., 1992. A theoretical analysis of interval drug dosing for cell-cycle-phase-specific drugs. Math. Biosci. 109, 85–97.

de Vladar, H.P., Gonzalez, J.A., 2004. Dynamic response of cancer under the influence of immunological activity and therapy. J. Theor. Biol. 227, 335–348.

Dyson, J., Villella-Bressan, R., Webb, G.F., 2002. Asynchronous exponential growth in an age structured population of proliferating and quiescent cells. Math. Biosci. 177/178, 73–83.

Jackson, T.L., Byrne, H.M., 2000. A mathematical model to study the effects of drug resistance and vasculature on the response of solid tumors to chemotherapy. Math. Biosci. 164, 17–38.

Kozusko, F., Bajzer, Z., 2003. Combining Gompertzian growth and cell population dynamics. Math. Biosci. 185, 153–167.

Kozusko, F., Chen, P., Grant, S.G., Day, B.W., Panetta, J.C., 2001. A mathematical model of in vitro cancer cell growth and treatment with the antimitotic agent curacin A. Math. Biosci. 170, 1–16.

Magni, P., Simeoni, M., Poggesi, I., Rocchetti, M., De Nicolao, G., 2006. A mathematical model to study the effects of drugs administration on tumor growth dynamics. Math. Biosci. 200, 127–151.

Norton, L., 2005. Conceptual and practical implications of breast tissue geometry: toward a more effective, less toxic therapy. Oncologist 10, 370–381.

Norton, L., Simon, R., 1977. Tumor size, sensitivity to therapy, and design of treatment schedules. Cancer Treat. Rep. 61, 1307–1317.

Norton, L., Simon, R., 1986. The Norton–Simon hypothesis revisited. Cancer Treat. Rep. 70, 163–169.

Norton, L., Simon, R., Brereton, H.D., Bogden, A.E., 1976. Predicting the course of Gompertzian growth. Nature 264, 542–545.

Panetta, J.C., 1996. A mathematical model of periodically pulsed chemotherapy: tumor recurrence and metastasis in a competitive environment. Bull. Math. Biol. 58, 425–447.

Panetta, J.C., 1997. A mathematical model of breast and ovarian cancer treated with paclitaxel. Math. Biosci. 146, 89–113.

Panetta, J.C., Kirstein, M.N., Gajjar, A.J., Nair, G., Fouladi, M., Stewart, C.F., 2003. A mechanistic mathematical model of temozolomide myelosuppression in children with high-grade gliomas. Math. Biosci. 186, 29–41.

Panetta, J.C., Webb, G.F., 1995. A mathematical model of cycle-specific chemotherapy. Math. Comput. Modell. 22, 67.

Parfitt, A.M., Fyhrie, D.P., 1997. Gompertzian growth curves in parathyroid tumours: further evidence for the set-point hypothesis. Cell. Prolif. 30, 341–349.

Pfreundschuh, M., Trumper, L., Kloess, M., Schmits, R., Feller, A.C., Rube, C., Rudolph, C., Reiser, M., Hossfeld, D.K., Eimermacher, H. et al., 2004a. Two-weekly or 3-weekly CHOP chemotherapy with or without etoposide for the treatment of elderly patients with aggressive lymphomas: results of the NHL-B2 trial of the DSHNHL. Blood 104, 634–641.

Pfreundschuh, M., Trumper, L., Kloess, M., Schmits, R., Feller, A.C., Rudolph, C., Reiser, M., Hossfeld, D.K., Metzner, B., Hasenclever, D. et al., 2004b. Two-weekly or 3-weekly CHOP chemotherapy with or without etoposide for the treatment of young patients with good-prognosis (normal LDH) aggressive lymphomas: results of the NHL-B1 trial of the DSHNHL. Blood 104, 626–633.

Ribba, B., Marron, K., Agur, Z., Alarcon, T., Maini, P.K., 2005. A mathematical model of Doxorubicin treatment efficacy for non-Hodgkin's lymphoma: investigation of the current protocol through theoretical modelling results. Bull. Math. Biol. 67, 79–99.

Sidorov, I.A., Hirsch, K.S., Harley, C.B., Dimitrov, D.S., 2003. Cancer treatment by telomerase inhibitors: predictions by a kinetic model. Math. Biosci. 181, 209–221.

Sullivan, P.W., Salmon, S.E., 1972. Kinetics of tumor growth and regression in IgG multiple myeloma. J. Clin. Invest. 51, 1697–1708.

Wheldon, T.E., 1988. Mathematical models in cancer research. Adam Hilger, Bristol, pp. 157–179.